FOREST FIRES IN PORTUGAL — CASE STUDY, 18 JUNE 2017

Milan M. RADOVANOVIĆ[1,2], Yaroslav VYKLYUK[3,12], Milan T. STEVANČEVIĆ[4], Milan Đ. MILENKOVIĆ[1], Dejana M. JAKOVLJEVIĆ[*1,5], Marko D. PETROVIĆ[1,2], Slavica B. MALINOVIĆ MILIĆEVIĆ[6], Natalia VUKOVIĆ[7], Aleksandra Đ. VUJKO[8], Anatoliy YAMASHKIN[9], Petro SYDOR[3], Darko B. VUKOVIĆ[10], Miroslav ŠKODA[11]

[1]Geographical Institute "Jovan Cvijić", Serbian Academy of Sciences and Arts, Belgrade, Serbia

[2]South Ural State University, Institute of Sports, Tourism and Service, Chelyabinsk, Russia

[3]Bukovinian University, Chernivtsi, Ukraine

[4]Former Federal Ministry of Telecommunication of Yugoslavia, Belgrade, Serbia

[5]Russian Institute for Advanced Study, Moscow State Pedagogical University, Moscow, Russia

[6]University Center for Meteorology and Environmental Modelling, University of Novi Sad, Novi Sad, Serbia

[7]Ural Federal University, Yekaterinburg, Russia

[8]Novi Sad Business School, Novi Sad, Serbia

[9]National Research Mordovia State University, Saransk, Russia

[10]Russian State Social University, Moscow, Russia

[11]DTI University, Department of Finance and Economics, Dubnica nad Váhom, Slovakia

[12]Wenzhou University, Institute of laser and optoelectronics intelligent manufacturing, China

[*] Dejana Jakovljević; E-mail: d.jakovljevic@gi.sanu.ac.rs

Forest fires that occurred in Portugal on 18 June 2017 caused several tens of human casualties. The cause of their emergence, as well as many others that occurred in Western Europe at the same time remained unknown. Taking into account consequences, including loss of human lives and endangerment of ecosystem sustainability, discovering of the forest fires causes is the very significant question. The heliocentric hypothesis has indirectly been tested, according to which charged particles are a possible cause of forest fires. We must point out that it was not possible to verify whether in this specific case the particles by reaching the ground and burning the plant mass create the initial phase of the formation of the flame. Therefore, we have tried to determine whether during the critical period, i.e. from 15–19 June there is a certain statistical connection between certain parameters of the solar wind and meteorological elements. Based on the hourly values of the charged particles flow, a correlation analysis was

performed with hourly values of individual meteorological elements including time lag at Monte Real station. The application of the Adaptive Neuro Fuzzy Inference System models has shown that there is a high degree of connection between the flow of protons and the analysed meteorological elements in Portugal. However, further verification of this hypothesis requires further laboratory testing.
Key words*: forest fires, heliocentric hypothesis, ANFIS models, Portugal*

1. Introduction

Forest cover more than one third of Portugal (3.2×10^6 ha), ranking eight in Europe as highest country with forestlands. Portugal also has the highest incidence of wildfire events in the Mediterranean basin, as well as in the whole Europe [1,2]. Large forest fires in Portugal during the last decades have caused loss of lives and huge burnt area. During the period 1980–2000 the mean burnt area by wildfires in Portugal was higher 9×10^4 ha per year [3]. The mean annual fire incidence was 3% of its forests and wildland surface area in the 2000–2011 [1]. During the summer fires in 2003, burnt area was approximately 4.5×10^5 ha and 20 people died [3]. The years 2003 and 2005 together registered over 7.5×10^5 ha burned, which is almost 9% of entire country [4]. Forest fire event in the north of Portugal on 14 October 2011 caused total of 4.4×10^3 ha of burnt area [5].

Regardless of catastrophic consequences, causes of forest fires often stay unknown. Taking into account detrimental effects of forests fires on sustainability of forest ecosystems, investigations of their causes are crucial. Many studies found that meteorological condition play fundamental role, both in ignition and during the fire spread [2,3,6]. Fire weather conditions (such as temperature, relative moisture, wind speed and drought factors) are the most critical factors in explaining many fire characteristics, spread, size and burn severity [7]. Other studies also confirmed correlation between forest fires and atmospheric condition [8–12].

In addition to numerous studies which describe influences of the solar activity on our atmosphere [13–17], examination of solar impact on forest fire occurrence becomes actual in recent years. As far as we know, Gomes and Radovanović [18] argue for the first time that the processes on the Sun could represent a potential explanation for the occurrence of forest fires. In the meantime, more research was published on this subject [19–24]. A new hypothesis attempts to link the processes on sun such as charged particles (protons and electrons) as potential causes of forest fires of unknown origin [25]. According to this hypothesis, this paper aims to present possible explanation for causes of forest fires in Portugal on 18 June 2017.

2. Materials and Methods

2.1. Theoretical background

Forest fires that occurred on 18 June 2017 in the central part of Portugal are among the most endangered in the history of this country. About 60 forest fires were reported during the night of 17/18 June 2017. The number of victims was 64, including 6 firefighters. Many died in their cars or near the vehicles when they tried to escape from the fire. About 200 people were injured. On 20 June, a plane with two crew members who participated in the extinguishing of the fire collapsed. On that day, the fires were localized. More than 4.5×10^5 ha of forest burnt.

A severe weather was mentioned as a possible reason. It is possible that the fire was caused by a thunderstorm, as the investigators found a tree that was hit by a "thunderstorm without rain", the Portuguese media reported, referring to police sources. In addition, some officials expressed the view that fires were deliberately set.

Gomes and Radovanović [26] presented a number of critical views on the so-called generally accepted attitudes regarding the explanation of the initial phase of the flame. In short, there was a suspicion of the possible responsibility of anthropogenic activity in 95% of cases, as it was accepted not only in the media, but also in many scientific circles. And first of all because it is hard to believe that, for example, over 30,000 fires have been reported over the years and the area of the burnt vegetation is over 3.5 x 10^6 ha (Figure. 1).

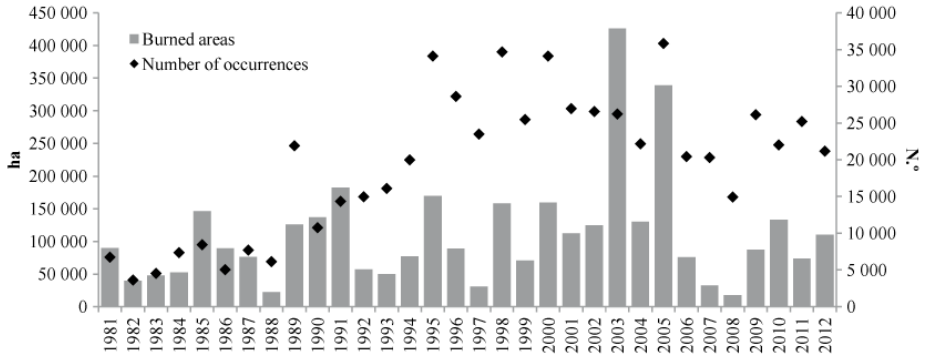

Figure 1. Evolution of the number of occurrences and burned area between 1981 and 2012 in Portugal [27]

Milenković et al. [28] found the connection between the number of forest fires in Portugal and the AMO. Considering the absolute values, there is a suspicion in some other so-called potential candidates, such as lightning or high air temperature. As for air temperature, it has been determined that a minimum of 300 ºC is required to show the initial phase of the flame [29]. This temperature has never been measured on the ground even closer (including desert areas), not to mention the air temperature.

According to the mentioned hypothesis, it is necessary to have a coronary hole and/or energy region in the geoeffective position on the Sun before the occurrence of a fire. On 15 June, the coronary holes CH807 and CH808, as well as the energy region 12663 were in the geoeffective position [30]. The maximum speed of the solar wind (SW) at La Grange Point was 594 km/s [31].

Radovanović and Stevančević [32] gave an interpretation of the SW propagation through the magnetosphere and the atmosphere. In the space between the Sun and the Earth, the current field moves along the lines of the magnetic field of the Sun, and in the free atmosphere, along the lines of the resulting magnetic field of the Sun and the Earth. The movement of charged particles creates a convection electric current, and the emergence of an electric current causes the appearance of a magnetic field in the form of a shell that does not allow the scattering of particles. The forces that occur in the current fields are the result of the interaction of the convection electric current and the magnetic field. The strength and direction of the electromagnetic force are uniquely determined by the vector product:

$$d\mathbf{F} = I d\mathbf{l} \times \mathbf{B}, \quad (1),$$

where I is the strength of the electric convection current, d**l** is the vector of the length of the current field and **B** is the magnetic induction vector.

Based on the eq. (1), it can be concluded that in the current field, the direction of positively charged particles (protons) is opposite to the direction of the negatively charged particles (electrons). The circulation of the charged particles in the current field is carried out in a level that is vertical to the direction of motion of the current field. The movement of the current field, that is the atmospheric river, is under the influence of the kinetic energy of the particles taken from the Sun. The moving of particles creates a convection electric current which creates a magnetic field. The magnetic field has the role of a shell that does not allow the particles to be scattered. However, during movement through the atmosphere, due to friction and increasing resistance of the geomagnetic field, there is a decrease in speed, which causes a decrease in the strength of the electric current. By reducing the electric current, the magnetic field strength decreases. At certain point, it comes to the magnetic shell breaking out, that is, the opening of the current fields, and the particles of the corpuscular radiation of the Sun enter the free atmosphere. After opening the current field, there is a spatial selectivity depending on the electrical load of the particles. The electrons move right and protons left of the direction of the radial velocity of the current field. After opening the current fields, the particles of corpuscular radiation enter the free atmosphere with a certain amount of motion [33].

The SW penetrates the Earth's atmosphere always at a certain angle θsw**,** which is the angle that the speed **v** makes with the vector of the magnetic induction **B**. We can separate the speed v into one component, vcos(θsw), in the directon of the magnetic field, and the other component, vsinθsw**,** perpendicular to the direction of the magnetic field. Then the result will be that the trajectory of the SW (which is the trajectory of the SW particles) is a spiral (helix), and the momentary diameter (eq. 2) of the cilinder around which the SW is spiraling is:

$$r = mv \sin(\theta sw)/qB \quad (2)$$

With increasing penetration into the lower layers of the atmosphere, there is an increasing effect of the geomagnetic field, that is, the effect of the circulation vector of the geomagnetic field, and the proton tube receives cyclone motion. The magnetic shell of the tube does not allow the scattering of particles, so the density of the particles increases with decreasing radius [34].

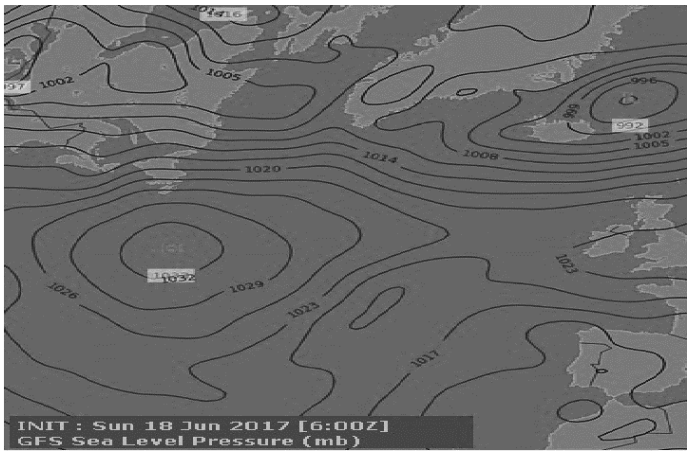

Figure 2. Synoptic situation on 18 June 2017 [35]. Over Portugal there is a zone with several separate locations of low air pressure (1011 mb) which according to theoretical approach suggest 3 relatively smaller penetrations of separate jets.

From the Figure 2 we can see the high pressure area over the Central Atlantic (1032) and the low pressure area above Iceland (996 mb). In that sense, Portugal has not registered such low pressure

as Iceland, but it is nevertheless significantly lower than over the central part of the Atlantic (the difference was over 20 mb). By evening, an area of 1011 mb covered the whole of Portugal, which is also referred to as a low-pressure region on the synoptic maps [36]. According to the model proposed by Gomes et al. [37], the penetration line, due to reconnection, was between Great Britain and Iceland. Two zones of high air pressure were formed south of this line, i.e. right of the direction of motion of the current field, the electron dissipation occurred, as it was previously theoretically shown. Left of this direction, the dissipation of protons dominates and the formation of the low air pressure field (Icelandic depression). Following this sequence of events, we come to the assumption that the fires that occurred simultaneously in Spain and France are the result of a wider dispersion of electrons of a different energy range [38]. However, in the case of Portugal, there is a penetration of the current field over the geomagnetic anomaly and, according to given hypothesis, this penetration has caused fires in Portugal. Only in the central part of Portugal there are densely grouped fires on a relatively small surface. As previously pointed out by Radovanović et al. [21], when the conditions are made for protons to reach the ground, due to their higher weight (in relation to electrons), they cause forest fires in smaller territories.

2.2. Calculations

Bearing in mind that it was not directly record the possible propagation of particles to the ground, as a potential cause, which causes the initial phase of the flame in the burning plant mass, we decided to test the heliocentric hypothesis indirectly. The following Hourly Averaged Real-Time data were used as the input parameters: Differential Electron (energy ranges 38–53 keV (E1) and 175–315 keV (E2)) and Proton Flux (energy ranges 47–68 keV (P1), 115–195 keV (P2), 310–580 keV (P3), 795–1193 keV (P4) and 1060–1900 keV (P5)) [39]; Integral Proton Flux (energy ranges > 10 MeV (I1) and > 30 MeV (I2)); Hourly Averaged Real-time Bulk Parameters of the Solar Wind Plasma Proton Density (W1) (p/cc), Bulk Speed (W2) (km/s) and Ion Temperature (W3) (K) [40]. ACE Satellite — Solar Wind Electron Proton Alpha Monitor is located at La Grange point so that it measures the data in real time that come from the Sun to our planet. Hourly meteorological data relating to Monte Real Station have been used as an output (Latitude: 39° 49' 52" N, Longitude: 8° 53' 14" W) [41]. This station is located in the military air-base, located near Leiria. The data include air temperature (°C), humidity (%) and air pressure (hPa). All data used in the paper refer to the period from 15–19 June 2017. This station was selected because it is located near the fire-affected area and the data are available on the Internet. The goal of calculations was to investigate the functional dependencies between the characteristics of the SW and air temperature — T, humidity — H and pressure — P. The solution of this problem consists of several stages.

2.2.1 Filling gaps

The feature of this Data Set is the presence of missed data (gap) with a maximum duration of 3 hours. The spline interpolation using not-a-knot end conditions was used to fill in these gaps. The interpolated value at a query point is based on a cubic interpolation of the values at neighbouring grid points in each respective dimension [42].

2.2.2 Correlation analysis

Correlation analysis was performed to establish the presence of a linear connection between the input and output fields (Table 1, where lag = 0 for the rows).

2.2.3 Lag analysis

To establish the lag dependence, the transformation of the Data Set was conducted. Output fields were fixed, after that the time series of each input field was shifted vertically downward by the number of rows equal to the lag studied. After that, the correlation coefficient between the input and output fields was calculated. We investigated the lag from 0 to 5 hours. The results of calculation are presented in the tab. 1.

Table 1. Correlation coefficients for lag transformation of Data Set

Lag	E1	E2	P1	P2	P3	P4	P5	I1	I2	W1	W2	W3
						Temperature (°C)						
0	−0.11	0.06	0.01	0.14	0.15	0.11	−0.10	−0.57	−0.55	−0.11	0.34	0.14
1	-0.05	0.09	0.06	0.14	0.22	0.16	−0.07	−0.58	−0.56	0.02	0.31	0.21
2	0.01	0.11	0.08	0.13	0.23	0.18	−0.06	−0.59	−0.57	0.13	0.28	0.26
3	0.03	0.14	0.09	0.12	0.21	0.18	−0.06	−0.59	−0.58	0.24	0.24	0.28
4	0.05	0.18	0.11	0.19	0.14	0.13	−0.06	−0.59	−0.58	0.34	0.21	0.30
5	0.08	0.19	0.08	0.22	0.10	0.08	−0.06	−0.59	−0.57	0.41	0.20	0.32
						Humidity (%)						
0	0.14	−0.02	−0.03	−0.12	−0.13	−0.08	0.06	0.50	0.48	0.16	−0.34	−0.12
1	0.04	−0.07	−0.08	−0.12	−0.21	−0.14	0.01	0.52	0.50	0.05	−0.32	−0.20
2	−0.01	−0.10	−0.12	−0.10	−0.22	−0.17	−0.01	0.52	0.50	−0.07	−0.28	−0.25
3	−0.05	−0.15	−0.13	−0.11	−0.19	−0.16	−0.02	0.52	0.51	−0.19	−0.23	−0.26
4	−0.08	−0.21	−0.13	−0.19	−0.12	−0.11	−0.03	0.53	0.52	−0.30	−0.19	−0.27
5	−0.07	−0.23	−0.12	−0.22	−0.07	−0.06	−0.04	0.53	0.52	−0.39	−0.16	−0.26
						Pressure (hPa)						
0	0.16	−0.17	0.11	−0.07	−0.17	−0.30	0.22	0.85	0.85	0.41	−0.47	−0.06
1	0.16	−0.17	0.07	−0.04	−0.20	−0.29	0.22	0.86	0.85	0.40	−0.48	−0.08
2	0.12	−0.16	0.08	−0.07	−0.22	−0.29	0.21	0.86	0.85	0.39	−0.51	−0.11
3	0.16	−0.18	0.06	−0.06	−0.24	−0.28	0.18	0.87	0.86	0.36	−0.52	−0.14
4	0.16	−0.20	0.01	−0.09	−0.25	−0.27	0.17	0.88	0.86	0.33	−0.55	−0.19
5	0.13	−0.18	0.01	−0.09	−0.25	−0.26	0.17	0.89	0.86	0.30	−0.56	−0.22

2.2.4 Autocorrelation analysis

For further research, an autocorrelation analysis should be carried out to reconcile the interconnection between the input fields. The results of these calculations are shown in the tab. 2.

Table 2. Autocorrelation coefficients for I1, I2, W1, W2, W3 input fields

	I1	I2	W1	W2	W3
I1	1.00				
I2	0.98	1.00			
W1	0.26	0.27	1.00		
W2	−0.55	−0.55	−0.29	1.00	
W3	−0.27	−0.28	0.14	0.73	1.00

2.2.5 Search of best models

As it can be seen from the lag correlation and autocorrelation analysis, the best models for all output fields must be dependence on integral proton flux and solar wind (eq. 3) with lag=5:

$$T(H, P)=F((I1 \text{ or } I2)_5, W1_5, W2_5, W3_5), \quad (3)$$

where subscribe index "5" means lag=5.

We must know which of them (I1 or I2) is better. Therefore we tested models $T(H,P)$=F(I15,W15, W25, W35) and $T(H,P)$=F(I25,W15, W25, W35) (tab. 3).

For checking this decision, the models with all possible combinations of lags from 0 to 5 were tested (64 = 1296 models). Models with I1 or I2 input fields were tested separately. The theoretical investigations [36] showed that electrons must have nonlinear impact on output fields. Therefore, similar calculations for models containing one of the fields E1 or E2 were carried out (65 = 7776 models). In addition, models that take into account only Differential Flux of electrons and protons were tested (67 = 279936 models). Linear regression analysis and Adaptive Neuro Fuzzy Inference System (ANFIS) were used as models in this investigation. Two Gauss membership functions (eq. 4) were created for each input field in ANFIS models:

$$f(x, \sigma, c) = e^{\frac{-(x-c)^2}{2\sigma^2}}, \quad (4)$$

where σ and c–obtained during the training of the neural network.

Since ANFIS is a Sugeno-type system, the output membership function type was checked as constant. Each ANFIS system was trained during 100 epochs, initial step size – 0.01, step size decrease rate – 0.9, step size increase rate – 1.1. Hybrid method was checked as optimization method used in membership function parameter training. For learning process Data Set was separated on training and test sets in proportion 90/10. This method is a combination of least-squares estimation and back-propagation.

Taking into account that 894,240 models have been investigated and all of them are independent on each other, the parallel calculation is used to solve this problem. It decreased time of calculation for about 3.5 times. The longest calculation lasted about 60 hours. The total time consisted of about 200 hours (~8 days). The results of these calculations are presented in the tab. 3.

Table 3. Comparison of correlation coefficients of the best models with models with lag=5 input fields

Models	Linear		ANFIS		Number of models	Position of (3) model (linear/ANFIS)
	Lag=5	Best	Lag=5	Best		
			Temperature			
F(I1, W1, W2, W3)	0.8199	0.8251	0.8529	0.8621	1296	19/16
F(I2, W1, W2, W3)	0.8113	0.8178	0.8483	0.8540	1296	11/11
F(I1, W1, W2, W3, E1)	0.8337	0.8431	0.8698	0.8839	7776	54/41
F(I1, W1, W2, W3, E2)	0.8239	0.8287	0.8843	0.9051	7776	65/359
F(E1, E2, P1, P2, P3, P4, P5)	0.3372	0.4241	0.3567	0.4733	279,936	95,927/196,615
			Humidity			
F(I1, W1, W2, W3)	0.7559	0.7680	0.8026	0.8247	1296	20/24
F(I2, W1, W2, W3)	0.7437	0.7597	0.7953	0.8115	1296	26/24

F(I1, W1, W2, W3, E1)	0.7705	0.7861	0.8216	0.8455	7776	46/123
F(I1, W1, W2, W3, E2)	0.7672	0.7831	0.8538	0.8910	7776	50/733
F(E1, E2, P1, P2, P3, P4, P5)	0.3553	0.4363	0.3689	0.4610	279,936	56,329/130,930
			Pressure			
F(I1, W1, W2, W3)	0.8985	0.9037	0.9483	0.9637	1296	178/247
F(I2, W1, W2, W3)	0.8767	0.8988	0.9338	0.9506	1296	932/512
F(I1, W1, W2, W3, E1)	0.8994	0.9055	0.9521	0.9679	7776	917/929
F(I1, W1, W2, W3, E2)	0.8991	0.9061	0.9576	0.9673	7776	1280/309
(E1, E2, P1, P2, P3, P4, P5)	*0.4090*	0.5879	0.4338	0.6153	279,936	256,184/276,420

3. Results

3.1. Correlation analysis

This section may be divided by subheadings. It should provide a concise and precise description of the experimental results, their interpretation as well as the experimental conclusions that can be drawn.

As you can see from the Table 2, Pearson correlation coefficients (*R*) are sufficiently small in all cases except I1 and I2. It means that any linear dependencies of these data are not observed. High values of *R* for I1 and I2 indicate the presence of strongly expressed nonlinear relationships. The presence of lagging (time) between the input and output fields may be another reason for the small correlation coefficients.

3.2. Lag analysis

As you can see from the tab. 1, the smallest *R* is observed for electron and proton flux (E and P). It means that these input fields do not impact on output fields for all lags. The largest *R* is observed for I1 and I2 relating to air pressure. As you can see *R* grows weakly with increasing lag. It means that there are nonlinear inertial dependencies between these fields and output fields. These lags mean that it is possible to make a prediction of output fields for few hours forward. Similar situation was observed for fields W1, W2, W3.

The results in the tab. 2 show strong linear relationship between I1 and I2 fields. It means that only one of them should be used in calculations.

3.3. Search of best models

As it can be seen from the tab. 3, correlation coefficient between real data and models' data was as criterion of accuracy. First of all, it should be noted that all ANFIS models have higher correlation coefficient than linear ones. It is clearly seen that models based on Differential Flux of electrons and protons have the smallest *R*. This means that they are not the main factors of influence on output fields.

Comparing models containing I1 and I2 factors allows us to conclude that the factor I1 makes it possible to better describe the output fields. It is true for Linear and ANFIS models.

As the calculations have shown, taking into account the factor describing Differential Flux of electrons allowed slight increase of the correlation coefficients for Linear and ANFIS models. It should be noted that the influence of factors E1 and E2 is approximately the same. Therefore, the factor E2 was chosen for further calculations.

So, in the next stage (eq. 5) we investigated the most accurate models:

$$T(H, P) = F(I1_l, W1_l, W2_l, W3_l, E2_l), \quad (5)$$

where l – lag.

As it can be clearly seen from the tab. 4, there is a large number of models that are more accurate than (3) (columns 2–3 and 4–5). As the last column of the model table shows, models (3) occupy far not the first places among the exact models. Therefore, the classical approach to the definition of exact models be equation (3), described in the stage lag analysis is not suitable for this class of tasks.

3.4. Accuracy analysis

To confirm this conclusion the adequacy of the three most accurate models was tested:

1) Linear with higher correlation coefficient,
2) ANFIS with higher correlation coefficient,
3) Model with higher total ($R_{\mathbf{Linear}} + R_{\mathbf{ANFIS}}$) correlation coefficient.

Information about input fields of these models is presented in the Table 5.

Table 5. Lags (equation 3) of the best models for forecasting T, H, P

Model	Best for:	$I1_l$	$W1_l$	$W2_l$	$W3_l$	$E2_l$	R
				Temperature			
T_1	Linear	1	5	0	0	5	0.8287
T_2	ANFIS	0	5	5	3	5	0.9051
T_3	Linear + ANFIS	5	5	2	3	5	1.7215
				Humidity			
H_1	Linear	1	5	0	0	5	0.7831
H_2	ANFIS	5	4	4	2	5	0.8910
H_3	Linear + ANFIS	4	5	5	3	4	1.6392
				Pressure			
P_1	Linear	4	3	3	3	4	0.9061
P_2	ANFIS	5	0	5	3	1	0.9673
P_3	Linear + ANFIS	5	0	5	3	0	1.8684

As it can be seen from the Table 5, the best linear model for Temperature is:

$$T_1 = F(I1_1, W1_5, W2_0, W3_0, E2_5).$$

The best ANFIS model is:

$$T_2 = F(I1_0, W1_5, W2_5, W3_3, E2_5).$$

The model with higher total correlation coefficient is:

$$T_3 = F(I1_5, W1_5, W2_2, W3_3, E2_5).$$

As it can be seen, lags of input fields of these models are different.

In addition, the lags of the input fields of these models are sometimes much smaller than in (3). On the other hand, it confirms that multimodels approach can make forecasting on different time periods from 0-5 hours.

According to the data for the lags from the Table 5, nine linear and nine ANFIS models were constructed:

$$T_1 = 195 - 88.8 \cdot I_1 + 0.58 \cdot W1_5 + 0.015 \cdot W2_0 - 1.96 \cdot 10^{-5} \cdot W3_0 + 4.43 \cdot 10^{-5} \cdot E2_5.$$

$$T_2 = 193 - 87.15 \cdot I_0 + 0.55 \cdot W1_5 + 0.072 \cdot W2_5 - 9.47 \cdot 10^{-6} \cdot W3_3 + 2.59 \cdot 10^{-5} \cdot E2_5.$$

$$T_3 = 220 - 98.7 \cdot I_5 + 0.56 \cdot W1_5 - 6.29 \cdot 10^{-4} \cdot W2_2 - 4.68 \cdot 10^{-6} \cdot W3_3 + 2.97 \cdot 10^{-5} \cdot E2_5.$$

$$H_1=-4.53+2.76\cdot I_1-0.02\cdot W1_5-8.79\cdot 10^{-4}\cdot W2_0+8.80\cdot 10^{-7}\cdot W3_0-2.12\cdot 10^{-6}\cdot E2_5.$$

$$H_2=-6.37+3.41\cdot I_5-0.014\cdot W1_4+4.08\cdot 10^{-4}\cdot W2_4-1.29\cdot 10^{-7}\cdot W3_2-1.75\cdot 10^{-6}\cdot E2_5.$$

$$H_3=-6.43+3.50\cdot I_4-0.019\cdot W1_5+1.34\cdot 10^{-4}\cdot W2_5+1.46\cdot 10^{-7}\cdot W3_3-1.48\cdot 10^{-6}\cdot E2_4.$$

$$P_1=888+64.47\cdot I_4+0.02\cdot W1_3+0.01\cdot W2_3+7.77\cdot 10^{-6}\cdot W3_3-1.39\cdot 10^{-5}\cdot E2_4.$$

$$P_2=886+65.05\cdot I_5-0.002\cdot W1_0-0.01\cdot W2_5+6.08\cdot 10^{-6}\cdot W3_3-8.60\cdot 10^{-6}\cdot E2_1.$$

$$P_3=886+65.07\cdot I_5-0.001\cdot W1_0-0.01\cdot W2_5+6.13\cdot 10^{-6}\cdot W3_3-1.57\cdot 10^{-5}\cdot E2_0.$$

After learning for each ANFIS model we got set of variables membership functions, rules, fuzzification and defuzzification methods, etc. [43]. For testing the accuracy of these models the results of model forecasting were compared with real data and correlation coefficient was calculated (Table 6).

Table 6. Pierson correlation coefficients of models from the Table (5)

Model	Linear	ANFIS
T_1	0.8287	0.8714
T_2	0.7697	0.9051
T_3	0.8204	0.9012
H_1	0.7831	0.8374
H_2	0.7076	0.8910
H_3	0.7629	0.8763
P_1	0.9061	0.9581
P_2	0.9010	0.9673
P_3	0.9032	0.9652

As it can be seen from the Table 6, all models have high *R*. All ANFIS models have higher correlation coefficient than linear ones. It confirms that ANFIS models are more accurate and take into account nonlinear effects. For a visual comparison of the results, the predicted values obtained by the models in comparison with the actual data are presented in the Fig. 3.

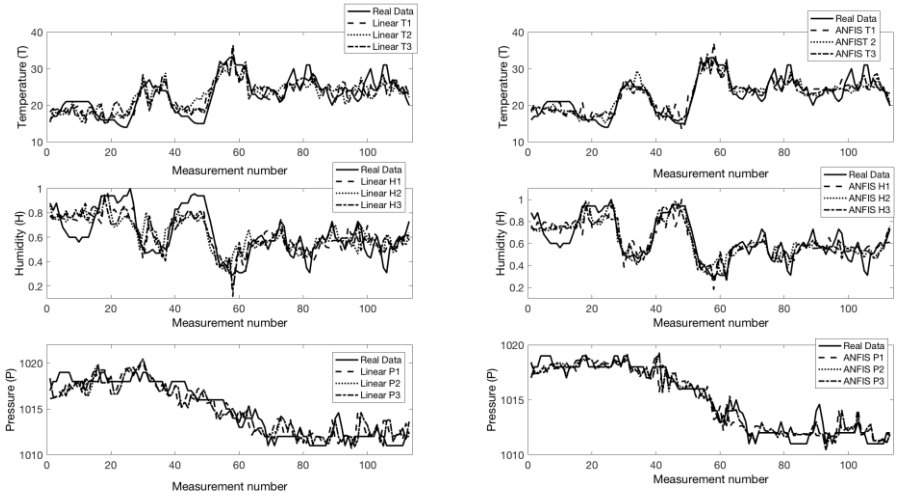

Figure 3. Comparison of the results, the predicted values obtained by the Linear and ANFIS models from the Tab. 6 in comparison with the actual data

3.5. Adequate analysis

As it can be seen from the figures, ANFIS models better describe and predict fluctuation in amplitude. It is clearly seen for Humidity models. Despite the high coefficient of ANFIS models, linear models also accurately describe the explored output fields. Therefore, an adequate analysis and sensitivity analysis is required to select the correct type of model.

For this purpose, for each model, the following calculation was made:

1) For each row of the training set, each value of the input parameter of turning was changed by 10%,
2) A relative change in the output field on change of separate input field was calculated,
3) Average data on all records.

As calculations showed 82% for linear T_1 means that in average if factor I1 increases on 10% the temperature will decrease on 82% after 1 hour (tab. 5). Similarly, the same increasing of I1 will lead to decreasing temperature after 5 hours on 57% accordingly to ANFIS model. As it can be seen, the most significant factors are I1 and W2. These results have also confirmed that electrons do not impact on investigated output fields. The results show that increasing I1 will lead to decreasing temperature and increasing humidity. In contrast, increasing W2 will lead to increasing temperature and decreasing humidity. It is clearly seen that input factors have weak impact on pressure despite the highest correlation coefficient of models.

4. Conclusions

Forest fires that occurred on 18 and 19 June 2017 in Portugal are among the most catastrophic ones of the country. As in many other cases, the cause of their emergence has remained unknown. Relying on the recent results, we have tried to test the heliocentric hypothesis of the occurrence of forest fires in this case. ACE satellite registered a sudden inflow of temperature, speed and density of the SW particles a couple of days before the formation of fires. The basic starting point was that if there is any connection between the process on the Sun and forest fires, then during critical days the meteorological parameters would have to “react” to some extent to certain parameters of the SW. In that sense, we have tried to determine whether there is any statistical connection between the flow of protons and electrons in some energy ranges on the one hand and the air temperature, relative humidity and air pressure in Monte Real on the other. The calculation included hourly values, but with a time lag shift from 0 to 5 hours in the period 15–19 June 2017. The largest R is observed for (I1) proton flux > 10 MeV and (I2) proton flux > 30 MeV (0.89 and 0.86 respectively) relating to air pressure.

Linear regression analysis and Adaptive Neuro Fuzzy Inference System (ANFIS) were used as models in this investigation. Taking into account that 894,240 models have been investigated and all of them are independent on each other, the parallel calculation is used to solve this problem. There are lots of models that can make forecasts of output fields with high level of accuracy. Nine linear and nine ANFIS models were constructed. ANFIS models are more accurate and take into account nonlinear effects.

The obtained results indicate the need of further improvement of the presented methods for the purpose of creation of scientifically based Web-oriented multimodels expert system for making forecasting of crisis events in different time periods from 0–5 hours. Especially if we have in mind

that, depending on the repeatability of certain processes in the Sun, we can expect more or less similar weather and environmental conditions in certain locations on Earth [44].

Other studies also found correlation between solar activity and forest fires. Velasco Herrera [19] found that the total solar irradiance minima provided the appropriate climatological conditions for the occurrence of Mexican forest fires. Sun et al. [45] concluded that fire growth was dependent on solar-driven winds. Kuznetsov and Baranovskiy [46] gave the new approach about possibility of forest fire ignition as result of focused sun's light.

Acknowledgment

This work was supported by the Ministry of Education, Science and Technological Development of the Republic of Serbia (project III 47007), Tomsk Polytechnic University (project No.14.Z50.31.0029 (19.03.2014)) and Russian Institute for Advanced Study, Moscow State Pedagogical University (MPSU Postdoctoral Fellowships in Humanities 2018).

References

[1] Botequim, B., *et al.*, Modeling post-fire mortality in pure and mixed forest stands in Portugal — A forest planning-oriented model, *Sustainability, 9* (2017), 3, pp. 390, DOI: 10.3390/su9030390

[2] Carvalho, A., *et al.*, The impact of spatial resolution of area burned and fire occurrence projections in Portugal under climatic change. *Clim Change, 98* (2010), 1–2, pp. 177–197, DOI: 10.1007/s10584-009-9667-2

[3] Pereira, M. G., *et al.*, Synoptic patterns associated with large summer forest fires in Portugal, *Agric For Meteorol, 129* (2005), 1–2, pp. 11–25, DOI: 10.1016/j.agrformet.2004.12.007

[4] Collins, R. D., *et al.*, Forest fire management to avoid unintended consequences: A case study of Portugal using system dynamics, *J Environ Manage, 130* (2013), pp. 1–9, DOI: 10.1016/j.jenvman.2013.08.033

[5] Monteiro, A., *et al.*, The EFFIS forest fire atmospheric emission model: Application to a major fire event in Portugal, *Atmos Environ, 84* (2014), pp. 355–362, DOI: 10.1016/j.atmosenv.2013.11.059.

[6] Guo, F., *et al.*, Understanding fire drivers and relative impacts in different Chinese forest ecosystems, *Sci Total Environ, 605–606* (2017), pp. 411–425, DOI: 10.1016/j.scitotenv.2017.06.219

[7] Lee, H. J., *et al.*, Complex relationships of the effects of topographic characteristics and susceptible tree cover on burn severity. *Sustainability, 10* (2018), 2, pp. 295, DOI: 10.3390/su10020295

[8] Hong, H., *et al.*, Applying genetic algorithms to set the optimal combination of forest fire related variables and model forest fire susceptibility based on data mining models. The case of Dayu County, China, *Sci Total Environ, 630* (2018), pp. 1044–1056, DOI: 10.1016/j.scitotenv.2018.02.278

[9] Hernandez, C., *et al.*, Impact of wildfire–induced land cover modification on local meteorology: A sensitivity studies of the 2003 wildfires in Portugal, *Atmos Res, 164–165* (2015), pp. 49–64, DOI: 10.1016/j.atmosres.2015.04.016

[10] Kane, V. R., *et al.*, Mixed severity fire effects within the Rim fire: Relative importance of local climate, fire weather, topography, and forest structure, *For Ecol Manage, 358* (2015), pp. 62–79, DOI: 10.1016/j.foreco.2015.09.001

[11] Slezakova, K., *et al.*, Forest fires in North Portugal: Impact on PM levels, *Atmos Res, 127* (2013), pp. 148–153, DOI: 10.1016/j.atmosres.2012.07.012

[12] Carvalho, A., *et al.*, Fire activity in Portugal and its relationship to weather and the Canadian Fire Index System, *Int. J. Wildland Fire, 17* (2008), 3, pp. 328–338, DOI: 10.1071/WF07014

[13] Nina, A., Čadež, V. Electron production by solar Ly-α line radiation in the ionospheric D-region, *Adv Space Res, 54* (2014), 7, pp. 1276–1284, DOI: 10.1016/j.asr.2013.12.042

[14] Nina, A., *et. al.*, The influence of solar spectral lines on electron concentration in terrestrial ionosphere, *Balt Astron, 20* (2011), 4, pp. 609–612, DOI: 10.1515/astro-2017-0346 448

[15] Bajčetić, J., *et. al.*, Ionospheric D-region temperature relaxation and its influences on radio signal propagation after solar X-flares occurrence, *Therm Sci, 19* (2015), Suppl. 2, pp. S299–S309, DOI: 10.2298/TSCI141223084B

[16] Nina, A., *et. al.*, Analysis of the relationship between the solar X-ray radiation intensity and the D-region electron density using satellite and ground-based radio data, *Sol Phys, vol. 293* (2018), Issue 4, article 64, pp. 1-19, DOI: 10.1007/s11207-018-1279-4

[17] Todorović Drakul, M., *et. al.*, Behaviour of electron content in the ionospheric D-region during solar X-ray flares, *Serb Astron J, 193* (2016), pp. 11–18, DOI: 10.2298/SAJ160404006T

[18] Gomes, J. F .P., Radovanovic, M, Solar activity as a possible cause of large forest fires a case study: Analysis of the Portuguese forest fires, *Sci Total Environ, 394* (2008), 1, pp. 197–205, DOI: 10.1016/j.scitotenv.2008.01.040

[19] Velasco Herrera, G., Mexican forest fires and their decadal variations, *Adv Space Res, 58* (2016), 10, pp. 2104–2115, DOI: 10.1016/j.asr.2016.08.030

[20] Radovanović, M. M., *et. al.*, Modelling of forest fires time evolution in the USA on the basis of long term variations and dynamics of the temperature of the solar wind protons, *Therm Sci, 19* (2015), 2, pp. S437–S444, DOI: 10.2298/TSCI141103150R

[21] Radovanović, M., *et. al.*, Application of ANFIS models for prediction of forest fires in the USA on the basis of solar activity, *Therm Sci 19* (2015), 5, pp. 1649–1661, DOI: 10.2298/TSCI150210093R

[22] Radovanović, *et. al.*, The influence of solar activities an occurrence of the forest fires in south Europe, *Therm Sci, 19* (2015), 2, pp. 435–446, DOI: 10.2298/TSCI130930036R

[23] Radovanović, M., *et. al*., Examination of the correlations between forest fires and solar activity using Hurst index, *J Geogr Inst Cvijic, 63* (2013), 3, pp. 23–32, DOI: 10.2298/IJGI1303023R

[24] Milenković, M., *et. al*., The impact of solar activity on the greatest forest fires of Deliblatska peščara (Serbia), *Forum geografic Studii şi cercetări de geografie şi protecţia mediului 10* (2011), 2, pp. 107–116, DOI: 10.5775/fg.2067-4635.2011.026.i

[25] Radovanovic, M. Solar activity, climate change, and natural disasters in mountain regions, in: *Sustainable Development in Mountain Regions* (Ed. G., Zhelezov), Springer International Publishing, Switzerland, 2016; pp. 9–19

[26] Gomes, J. F. P., Radovanovic, M, *Solar Activity and Forest Fires.* Nova Science Publishers, New York, USA, 2009

[27] ***, ICNF, https://mediterranee.revues.org/docannexe/image/6863/img-1.png

[28] Milenković, M., *et. al.*, Forest fires in Portugal — the connection with the Atlantic Multidecadal Oscillation (AMO), *J Geogr Inst Cvijic 67* (2017), 1, pp. 27–35, DOI: 10.2298/IJGI1701027M

[29] Viegas, D. X., A mathematical model for forest fires blowup, *Combust Sci Technol*, 177, (2004), pp. 27–51, DOI: 10.1080/00102200590883624

[30] Alvestad, J., Solar Terrestrial Activity Report, http://www.solen.info/solar/old_reports/2017/june/20170616.html

[31] Alvestad, J., Solar Terrestrial Activity Report, http://www.solen.info/solar/indices.html

[32] Radovanović, M., Stevančević, M. Exchange of energy between the Sun and outer space, in: *Energy Science and Technology* (Eds. U.C., Sharma *et al.*), Studium Press LLC, Houston, USA, 2015, pp. 264–282

[33] Radovanović, M., Forest fires in Europe from July 22 to 25, 2009, *Arch Biol Sci, 62* (2010), 2, pp. 419–424. DOI: 10.2298/ABS1002419R

[34] Mukherjee, S., Radovanović, M., Influence of the Sun in the genesis of tornadoes, *The IUP Journal of Earth Sciences, 5* (2011), 1, pp. 7–21

[35] ***, Metcheck, http://www.metcheck.com/WEATHER /gfscharts_archive.asp.

[36] ***,Wetterzentrale,http://www.wetterzentrale.de/reanalysis.php?jaar=2017&maand=6&dag=18&uur=000&var=45&map=1&model=nws.

[37] Gomes, J. F. P., *et al.*, Wildfire in Deliblatska Pescara (Serbia) — Case Analysis on July 24th 2007, in: *Forest Fires: Detection, Suppression and Prevention* (Eds. E. Gomez, K. Alvarez), Nova Science Publishers, New York, USA, 2009, pp. 89–140

[38] Radovanović, M., *et al.*, Electrons or protons: what is the cause of forest fires in Western Europe on June, 18 2017?, *J Geogr Inst Cvijic, 67* (2017), 2, pp. 213–218, DOI: 10.2298/IJGI1702213R

[39] ***, Space Weather Prediction Center, National Oceanic and Atmospheric Administration, ftp://ftp.swpc.noaa.gov/pub/lists/ace2/201706_ace_epam_1h.txt

[40] ***, Space Weather Prediction Center, National Oceanic and Atmospheric Administration, ftp://ftp.swpc.noaa.gov/pub /lists/ace2/201706_ace_swepam_1h.txt

[41] ***, Weather Underground https://www.wunderground.com/history/airport/LPMR/2017/6/15/DailyHistory.html?req_city=&req_state=&req_statename=&reqdb.zip=&reqdb.magic=&reqdb.wmo=

[42] Hazewinkel, M., *Encyclopaedia of Mathematics: Monge — Ampère Equation — Rings and Algebras*, Springer, 2013

[43] Jang, J-SR, ANFIS: adaptive-network-based fuzzy inference system, *IEEE Transactions on Systems, Man, and Cybernetics, 23* (1993), 3, pp. 665–685, DOI: 10.1109/21.256541

[44] Todorović, N., Vujović, D, Effect of solar activity on the repetitiveness of some meteorological phenomena, *Adv. Space Res.* (2014), *54*, 2430–2440. DOI: 10.1016/j.asr.2014.08.007

[45] Sun, R., *et al.*, The importance of fire-atmosphere coupling and boundary-layer turbulence to wildfire spread, *Int J Wildland Fire, 18* (2009), 1, 50–60, DOI: 10.1071/WF07072

[46] Kuznetsov, G. V., Baranovskiy, N. V., Focused sun's rays and forest fire danger, *Proceedings* of SPIE, Remote Sensing of Clouds and the Atmosphere XVIII; and Optics in Atmospheric Propagation and Adaptive Systems XVI, International Society for Optics and Photonics, 2013